

low as $0.62 \sim 14 \times 10^{-3}$ SI units while areas containing magnetite have a high value of 75×10^{-3} SI units. In the Las Palmas alteration zone, anomalous zones ($0.1 \sim 3 \times 10^{-3}$ SI units) are widely distributed and well coincide with the occurrence of alteration zones. Mineralized zones in three places in the southern part of the Las Palmas alteration zone are also included in anomalous zones ($0.37 \sim 20 \times 10^{-3}$ SI units). The Cochapamba alteration zone is included in anomalous zones ($0.3 \sim 3 \times 10^{-3}$ SI units) found over a wide range of area. These anomalous zones also include low susceptibility zones resulting from quartz-bearing andesite lava, tuffs, and sedimentary rocks of the Macuchi Formation.

As described above, magnetic susceptibility measurement was highly effective in understanding characteristics and scale of mineralization and alteration.

1-1-5 Geochemical Survey

(1) Collection of Samples, Components for Analysis and Analysis Method

The purpose of this work is to identify elements which are involved in mineralization of rocks in the vicinities of mineralized zones and to investigate the dispersion of these elements. For geochemical survey, 33 rock samples were obtained and analyzed for the seven elements of Ag, Cu, Pb, Zn, Mo, Co and Ni by inductively coupled argon plasma emission spectrochemical analysis (ICP). Detectable limit of these elements in analysis is 0.1ppm for Ag and 1ppm for the other six elements.

(2) Data Processing

A total of 67 rock samples including 34 samples collected in the other areas to be described later were analyzed for the seven elements. Results of this analysis were input to computer along with geological units at the sampling points for statistical data processing. Results of analysis are as shown in Table A-6. To meet the above objects, multivariate analysis rather than univariate is a more effective analysis method.

Multivariate analysis comes in various methods. Among them, factor analysis is effective as an analysis method which is designed to explain variations represented by multiple variables using a much fewer representative, hypothetical variations (factors), thereby scientifically attaining simplicity. To explain relationships of each sample with mineralization or characteristics of host rock, this method indicates which factor approximately in what quantity the sample has by assigning factor score to each sample.

For computation, computer was used and data were processed by varimax rotation, one of factor analysis methods. As a result, four factors were identified, namely (1) Co-Ni-Zn, (2)

Ag-Cu, (3) Pb-Zn-Cu and (4) Mo. Table II-1-3 shows a correlation matrix between elements, Table II-1-4, factor loading, communality and factor contribution as identified by factor analysis, and Table A-6, the factor score of each factor for each sample.

Among the existing geochemical survey data, those dealing with rocks number 85 reports. However, these reports were used only as supplementary data because analysis in these reports was limited to the four elements of Cu, Pb, Zn and Mo.

(3) Interpretation Results

More than 1 points earned in absolute value for each factor was rated as a high factor score, more than 0.4 and less than 1 as a medium factor score, and more than 0.0 and less than 0.4 as a low factor score.

Samples which earned high to medium factor scores in the second factor (Ag-Cu) were all of rocks in the Macuchi Formation. Samples with low factor scores were found in part of granodiorite in the El Torneado mineralized zone. Thus, this factor is considered reflecting characteristics of host rock and some Zn addition.

Samples which earned high to medium factor scores in the second factor (Ag-Cu) were obtained from the El Torneado, Osohuayco, and El Cristal mineralized zones as well as such zones in downstream of Palmas valley. Samples with low factor scores were found in the Las Juntas mineralized zone and the Cochapamba alteration zone (Fig. II-1-7). According to existing data, although some of sampling points were different, anomalous Cu zones cover the El Torneado, El Cristal and Las Juntas mineralized zones. This factor is considered characterizing Ag-Cu mineralization.

Samples with high to medium factor scores in the third factor (Pb-Zn-Cu) showed no difference between rocks. Generally speaking, there may be some areal difference because samples with high to medium factor scores were rather concentrated in part of El Torneado, and the Telimbela and San Miguel areas to be described later. It is difficult to estimate the process that characterizes this factor but younger mineralization process involving sulfide minerals as seen in, for example, the San Miguel area can be considered responsible for this factor.

Samples which earned high to medium scores of the fourth factor (Mo) were found in the El Torneado and El Cristal mineralized zones and the Las Palmas alteration zone (Fig. II-1-7). However, these samples were obtained from points different from those for samples with high to medium second factor scores, with some exception. The El Torneado mineralized zone shows a phenomenon that sulfide mineral-quartz networked veins containing molybdenite in the latter period cut sulfide mineral disseminated zones. From this phenomenon, this factor is considered

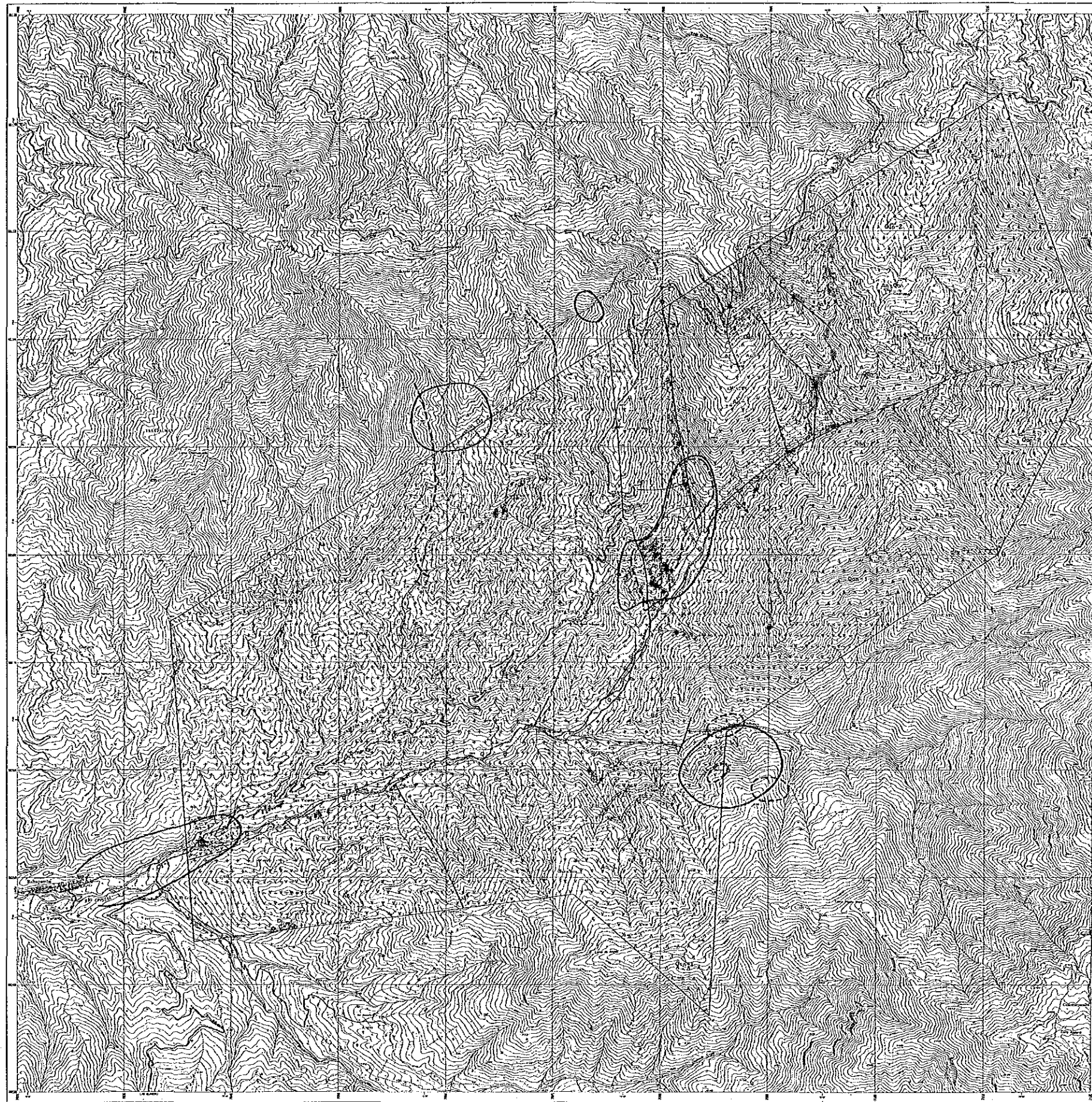
Table II-1-3 Correction Matrix of Each Element of Geochemical Data

	Ag	Cu	Pb	Zu	Mo	Co	Ni
Ag	1						
Cu	0.482	1					
Pb	0.096	0.154	1				
Zu	0.059	0.246	0.108	1			
Mo	0.096	0.129	0.043	-0.113	1		
Co	0.081	0.227	0.091	0.420	-0.064	1	
Ni	0.233	0.293	-0.043	0.342	0.009	0.587	1

Table II-1-4 Results of Factor Analysis of Geochemical Data

	Factor Loadings (varimax rotation)				Communality
	Factor 1	Factor 2	Factor 3	Factor 4	
Ag	-0.076	0.686	0.045	-0.133	0.4958
Cu	-0.238	0.616	0.253	-0.095	0.5086
Pb	-0.018	0.083	0.396	-0.041	0.1659
Zn	-0.473	0.114	0.275	0.335	0.4248
Mo	0.040	0.110	0.052	-0.345	0.1355
Co	-0.765	0.046	0.121	0.084	0.6091
Ni	-0.737	0.246	-0.130	-0.015	0.6203
Factor Contributions	62.150%	27.292%	10.191%	4.559%	

BALZAPAMBA



LEGEND

- | | | |
|----------------------------------|---------------------------------|---|
| Quaternary | Q | Gravel, sand, clay |
| | Qan-2 | Quartz-bq. andesite lava with its pyroclastics (H Member) |
| | An-3 | Alteration of andesite and quartz-bq. andesite lavas with their pyroclastics (E Member) |
| | An-3 | Andesite lava with quartz-bq. andesite lava (D Member) |
| | Tf | Andesite to quartz-bq. andesitic pyroclastics (D Member) |
| | An-2 | Andesite lava (C Member) |
| | Qan-1 | Quartz-bq. andesite lava with its pyroclastics (B Member) |
| Cretaceous Macabiti Formation | An-1 | Andesite lava with its pyroclastics and sediments (Tf), and hornfels (A Member) |
| | Gd | Granodiorite |
| | Di | Meltonocratic diorite dyke |
| | Tt | Trachyandesite dyke |
| Intrusive Rocks | Ap | Aplite dyke |
| | Dip and strike of bedding plane | |
| | Geological boundary | |
| | Fault | |
| Anticlinal axis | | |
| Synclinal axis | | |
| Mineralized zone (Presumed) | | |
| Vein | | |
| Alteration zone | | |
| Section line | | |
| + Location of geochemical sample | | |
| Factor 2 (Ag-Cu) | | |
| ○ F2 ≥ 1.0 | | |
| ○ 0.4 ≤ F2 < 1.0 | | |
| ● 0.0 ≤ F2 < 0.4 | | |
| Factor 4 (Ni) | | |
| □ F4 ≤ -1.0 | | |
| □ -1.0 < F4 ≤ -0.4 | | |
| ■ -0.4 < F4 ≤ -0.0 | | |
| Previous data | | |
| ○ Cu anomaly (146-38,200ppm) | | |
| ○ Mo anomaly (15-20,000ppm) | | |



Fig. II-1-7 Interpretation Map of Geochemical Data of the Balzapamba Area

to be a factor suggesting mineralization containing Mo that has taken place after mineralization containing Cu.

1-1-6 Discussion

Mineralization in the Balzapamba area includes the three types of porphyry copper, vein and hot spring. In the El Torneado and Osohuayco mineralized zones of porphyry copper type, mineralized zones extends in NNE-SSW to NE-SW directions. These directions are consistent with the directions of NNE-SSW to NE-SW system tectonic lines that develop in the northern and southern part of the Bolivar area. This fact, combined with the NE-SW trend of distribution of granodiorite mass in the balzapamba area, suggests that there may be genetical relationship between tectonic movement and intrusion of granodiorite as well as further subsequent hydrothermal activities. The mineralized zones are distributed in the peripheral zones of granodiorite mass and mineralization extends up to adjacent the Macuchi Formation. This fact indicates that the peripheral areas of granodiorite mass are favorable for ascending of hydrothermal fluids.

Hydrothermal activities in the Bolivar area can broadly be divided into three stages (Fig. I-4-1). Mineralizations of both porphyry copper type and vein type are formed by the first stage hydrothermal activity accompanied by sulfide minerals. In the El Torneado mineralized zone, disseminated mineralized zones are intersected with networked vein mineralized zones. From this fact, the mineralization in the Balzapamba area can be further subdivided into two stages of dissemination and networked veins. In the networked veins, sulfide minerals-chlorite-quartz networked veins intersect sericitized and silicified zones of host rocks, and further late quartz veins accompanied by molybdenite cut chalcopyrite-pyrite-chlorite veins, and magnetite occurs together with sulfide minerals in networked veins. These facts suggest that network mineralization itself also consists of several stages of hydrothermal activities under the circumstances of change in chemical composition of hydrothermal fluids and change of environment from reduction to oxidation. Scheelite occurs in networked veins of the El Torneado mineralized zone. This is a noteworthy fact because it closely resembled mineral assemblage of porphyry-molybdenum mineralization of quartz monzonite type classified by White et al (1981). However, the relationship between copper and molybdenum mineralizations should be investigated more detail because molybdenum-bearing quartz veins intersect copper-bearing secondary biotite-chlorite-quartz veins, and chalcopyrite-pyrite-chlorite veins cut molybdenite disseminated zones in the alteration zone. The detection of the factors related to copper and molybdenum mineralizations by geochemical survey is considered to suggest the presence plural stage of mineralization.

Furthermore, it is a subject for further study to determine whether mineralization in the El Cristal mineralized zone and that in San Miguel are formed in the same stage or in another stages.

The Las Palmas and Cochapamba alteration zones are characterized by acid hydrothermal alteration (silica-kaolinite-halloysite), silicification with leaching and occasional appearance of hematite-(silica sinter)-clay networked vein zone. These alteration are quite similar to that observed in the Lourdes Volcanic Rocks of the San Miguel area which correspond to the alteration episode of the second stage hydrothermal activity in the Bolivar area. Furthermore, alteration zone of this type is observed as horizontal layers in unaltered host rocks in outer zone of the Las Palmas alteration zone. This indicates a remnant of lateral current of hydrothermal solution.

1-2 Geophysical Survey

1-2-1 Purpose of Survey

The CSAMT survey was carried out in Balzapamba which was delineated as a high mineral potential area in a previous survey, in order to clarify the underground resistivity distribution, to extract the promising zone for occurrence of ore deposits and to assist in the location of an exploratory drilling site.

Although the topography of the survey area is comparatively steep and its altitude range from 800 to 3,000m, the survey was completed on schedule covering an area of 36km² with 104 observed stations.

1-2-2 Survey Method

(a) Methodology of CSAMT

The CSAMT (Controlled Source Audio-frequency Magneto-telluric) method was introduced by Goldstein (1971) and Goldstein and Strangway (1975) to overcome the problems encountered by the audio magnetotelluric (AMT) and magnetotelluric (MT) methods.

The MT method is a well known exploration technique, used widely in hydrocarbon and geothermal exploration. MT measures fluctuations in the earth's natural electric and magnetic fields, in a broad range of frequencies between about 0.0005 Hz and 100 Hz. When the measurements are made in the audio-frequency range (10 Hz to 20 KHz), the method is known as Audio-frequency Magnetotellurics (AMT). Neither MT nor AMT requires a man-made power source. However, advantages of this method are often negated by the low magnitude and high variability of the natural signals.

In the CSAMT method the controlled current is transmitted by a remote grounded bipole and both the electric field (E-field) and magnetic field (H-field) are measured in the survey area far from the current source.

The penetration depth of an electromagnetic wave is a function of the earth's resistivity and the frequency of the wave, which is expressed by the following equation:

$$d=503\sqrt{\rho/f}$$

d : skin depth (m)

ρ : apparent resistivity ($\Omega \cdot m$)

f : frequency (Hz)

In this equation, d is called the skin depth and show the depth, at which the magnitude of the electromagnetic field decreases about 37% to that on the surface. The above equation indicates also that lower frequencies can penetrate to a greater depth, allowing deeper investigation. The earth's resistivity is given by the well known Cagniard equation, which uses the magnitude of the measured E-field and H-field at any frequency when the distance from a source to a receiver location is longer than three times the skin depth.

$$\rho_a = 1/5f \cdot |E/H|^2$$

ρ_a : apparent resistivity ($\Omega \cdot m$)

E_x : electric field (mV/km)

H_y : magnetic field (gamma)

Measurement of a broad range of frequency of electromagnetic field leads to a determination of resistivity change as a function of depth.

(b) Field Procedure

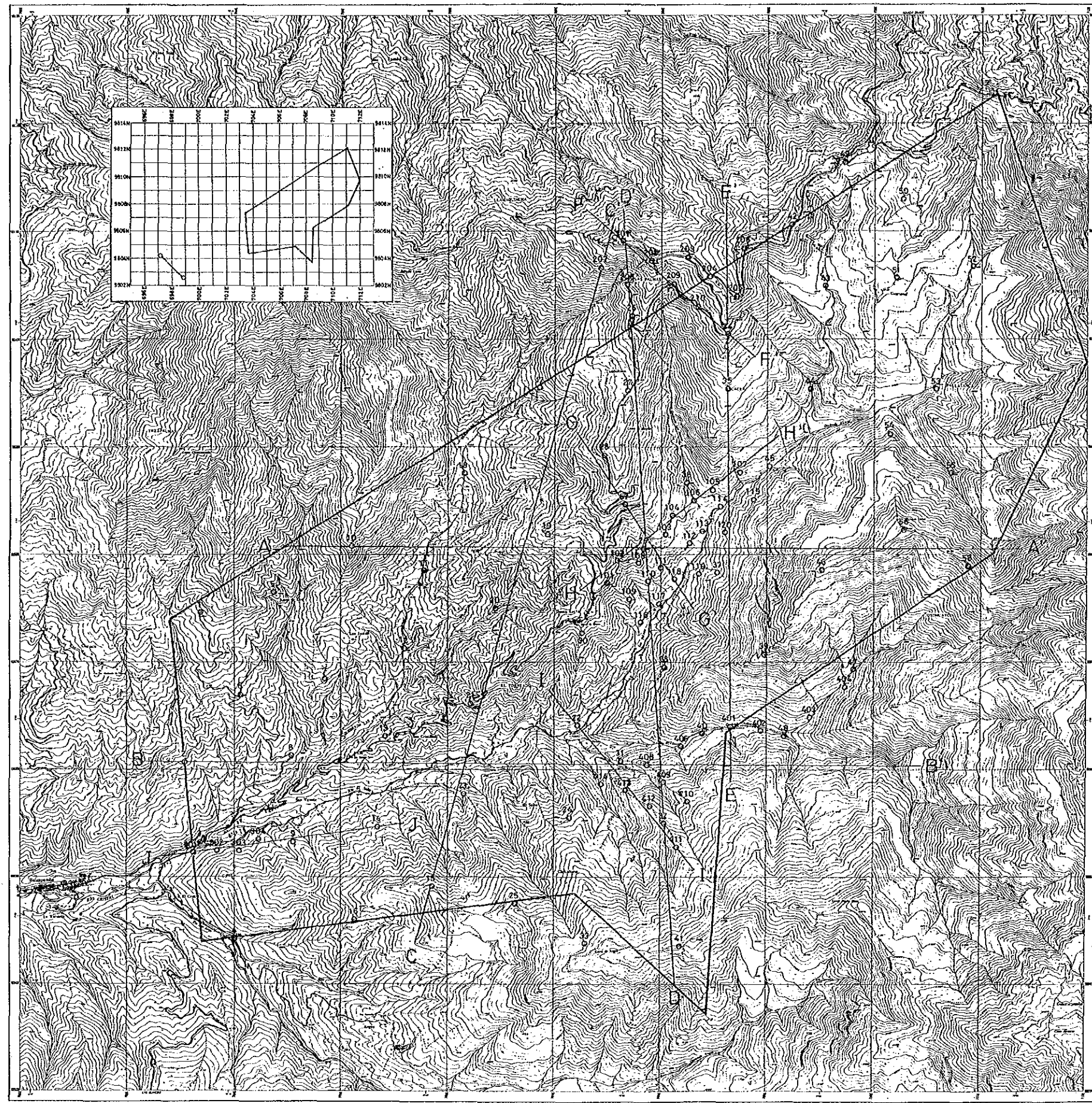
Current was sent through a grounded bipole of about 2.0 km length placed along El Vergel river about 5 km southeast of the survey area, to detect the electromagnetic fields as plane waves at receiver site. The orientation of the bipole was N47°W. Although the distance between the transmitter and receiver exceeded 8 km in the northeastern part of the area, the location of the grounded bipole was not moved because of the strong received signal.

Fifty eight observation stations were set covering the survey area of 36km² and then 46 stations were set in the four areas where mineralizations were found as the detail survey after general survey of 58 stations (Fig. II-1-8).

Both the E-field and H-field are measured at the frequency transmitted from the remote bipole source. Fig. II-1-9 illustrates Schematic Map of CSAMT Survey. The E-field was measured by a 50m dipole using a non-polarizable electrodes oriented parallel to the transmitter bipole. The H-field was measured by a horizontal magnetic sensor coil placed on the ground, approximately at the center of the E-dipole. It should be placed several meters away from the E-dipole line and receiver console to avoid interference, as well as to reduce inductive coupling due to operator movement.

Both the measured E-field and H-field as well as their relative phase are digitally stacked, filtered and processed in real-time and the apparent resistivity is simultaneously calculated by the above Cagniard equation at each frequency. The processed data are transferred and stored in RAM memory of data recorder linked to the receiver. The observation was done at least three

BALZAPAMBA



LEGEND

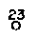
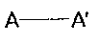

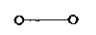
-  Station and No.
-  Section
-  Survey Area
-  Current Electrode



Fig. II - 1 - 8 Location Map of Observed Stations of CSAMT Survey

times for every frequency until reliable data were obtained. The followings are contents of data block stored in the memory.

ST : Station Number
FRQ : Frequency Code
HZ : Frequency
GAINS : Binary Gain
FILTER : Notch Filter
STKS : Stacking Times
A-SP : Dipole length
COIL : Coil Channel
GAIN : Gain of Coil Sensor
CRNT : *Transmitter Current (Ampere)*
ME : Measured Electric Potential (Volt)
PE : Phase of E-field (radian)
MH : Measured Magnetic Potential (Volt)
PH : Phase of H-field (radians)
E : *Magnitude of E-field (Volt/meter)*
H : *Magnitude of H-field (Kilo gramma)*
RHO : Cagniard Apparent Resistivity ($\Omega \cdot m$)
PD : Phase Difference of E-field and H-field (radian)

In this survey, 10 frequencies in the AMT range were used to get enough depth information, namely,

4, 8, 16, 32, 64, 128, 256, 512, 1,024, and 2,048 Hz.

The apparent resistivity curve is made by plotting the observed resistivities and frequencies in logarithmic scale.

(c) Instrumentation

The survey was carried out by using an CSAMT system manufactured by Zonge Engineering & Research Organization, Inc (U.S.A) which is able to measure E-field and H-field as well as their phases at every frequency.

The instruments were as follows:

1) Transmitter System

a) Engine generator (ZMG-20)

Output 20 KV, 400 Hz

b) Transmitter (GGT5)

Maximum output 10 KW
Maximum output current 10 A
Maximum output voltage 1,000 V

c) Transmitter Controller (XMT-12)

Frequency range 1 ~ 2,048 Hz

2) Receiver System

a) Data processor (GDP-12/2GB)

Frequency range 1 ~ 2,048 Hz
A/D converter, 50/60 Hz notch filter and 16 K byte RAM
Minimum input voltage 0.2 microV

b) Data recorder (DR-1)

500 Kbyte RAM, RS-232C interface

c) Antenna Coil (AN2)

2 axes ferrite coil
Coil sensitivity 0.2 mV/gamma

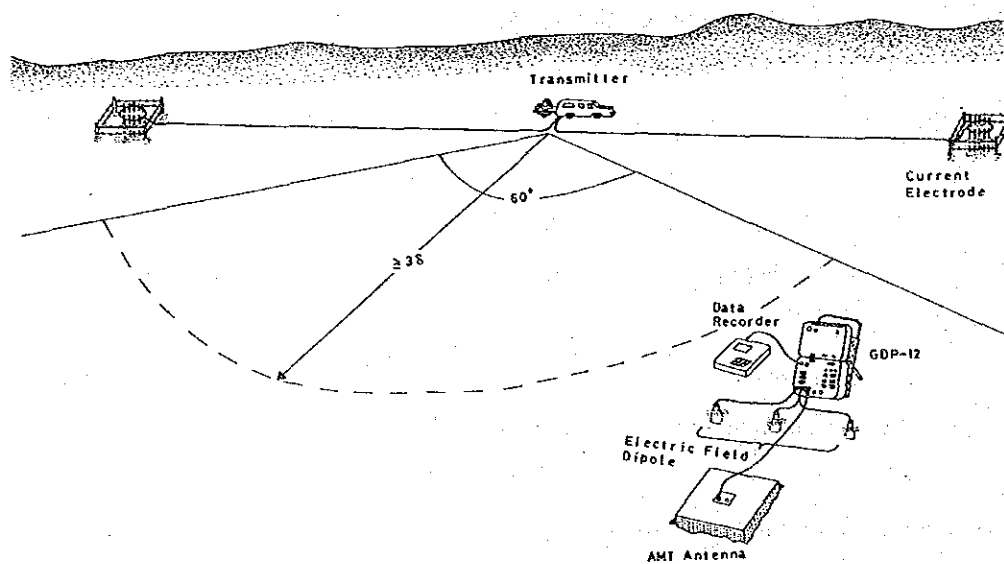


Fig. II-1-9 Schematic Map of CSAMT Survey

1-2-3 Data Analysis

The apparent resistivity is calculated from the ratio of the E-field and H-field magnitude by the above mentioned Cagniard equation. It should be noted that this equation is exactly valid only in the plane wave region of the electromagnetic field; i.e., only when the distance between transmitter and receiver location is sufficiently large. In the CSAMT survey, that distance is constrained, in general, by the requirement that the E-field and H-field be strong enough to permit useful measurements. The paradox encountered is that where the "plane wave" assumption is valid, the signal may be weak; and where the signal is strong (near the transmitter), the "plane wave" assumption is no longer valid.

If the distance between transmitter and receiver is much less than the three times of the skin depth, the field detected is not "plane wave" in character; it is referred to as the "near field". In the "near field", the Cagniard equation overestimates the actual resistivity. Fig. II-1-10 shows the apparent resistivity curve, using the Cagniard equation with theoretically calculated E_x and H_y values, over a homogeneous earth. The apparent resistivity curve in the "near field" is characterized by a slope of 45 degrees, meaning that the apparent resistivity value is doubled by each binary frequency step. The area of the gradual change between "far field" and "near field" is called "transition zone".

Since the earth is not homogeneous, the apparent resistivity obtained for each frequency does not represent the true underground resistivity. Therefore, to analyze the underground resistivity structure, one-dimensional multi-layered structure analysis is first carried out taking into account the "near field" effect. Namely, a initial theoretical curve which is calculated by assuming a layered model and using the exact coordinate location of the receiver and the transmitter is to be matched by trial and error to the observed data, then a least square iteration technique is adopted to determine the most suitable layered model. This calculation was done by using a computer program which calculates the electric and magnetic fields about a grounded horizontal electric dipole over a horizontally stratified earth. By inversion technique our program matches the sounding curve theoretically computed to the observed data.

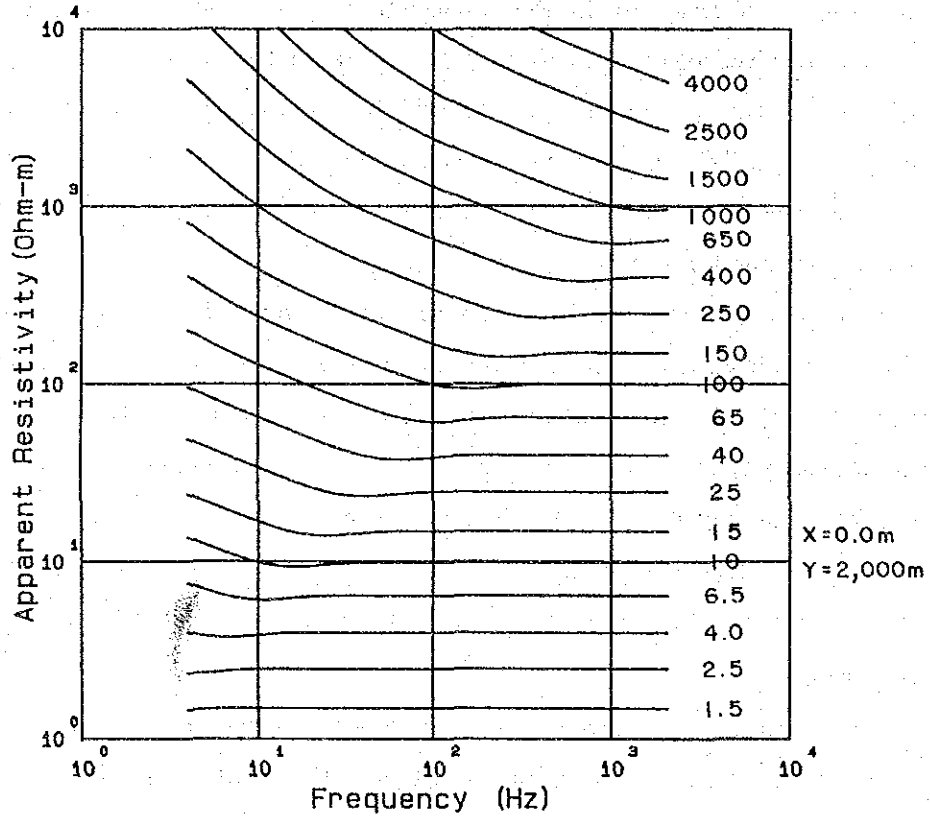


Fig. II - 1 - 10 Example of the Curve by 1-D Analysis

1-2-4 Results of Survey and Analysis

(1) Results of Measurement of Rock Samples

Although it is difficult to uniformly associate rocks classified by geology with their resistivity; fresh igneous rocks, metamorphic rocks, etc. generally have a high level resistivity, indicating more than $10,000 \Omega \cdot m$ as shown in Table II-1-5. This resistivity may substantially vary depending on the extent of weathering.

Geology of the survey area is classified into two types. One is the Macuchi Formation and other is granodiorite. The Macuchi Formation consists of andesite lava, its tuff, quartz bearing andesite lava and its tuff, which is partly metamorphosed to hornfels by granitic intrusion.

Rock samples collected from the survey area and cores from the drill holes MJE-1, 2 and 3 were measured at laboratory for their electrical properties (resistivity, FE). Those results show that silicified rocks, hornfels and granodiorite have a high resistivity (5,000 to more than $10,000 \Omega \cdot m$). Quartz bearing andesite lava, its tuff, as well as andesite lava and granodiorite subjected to weathering or alteration have a medium resistivity (1,000 to $1,500 \Omega \cdot m$) while andesite tuff have a low resistivity (less than $1,000 \Omega \cdot m$), drilling cores (granodiorite) containing sulfides are generally lower in resistivity than fresh rocks.

The resistivities of rock samples tends to be higher than those measured in the field. When comparative study is made on results of electrical property tests, on the resistivity values of the surface layer (the first layer) obtained by one-dimensional resistivity analysis for each measuring point, and on the type of rocks distributed there, the resistivity of rocks in the survey area can broadly be classified as shown below. The resistivity may also vary depending on the degree of cracks in rocks and the nature of underground water filling these cracks.

Andesite lava metamorphosed to hornfels	More than $10,000 \Omega \cdot m$
Fresh granodiorite and fine-grained granodiorite	$5,000 \sim 10,000 \Omega \cdot m$
Rock subjected alteration such as chloritization	$1,000 \sim 1,500 \Omega \cdot m$
Macuchi Formation (except hornfels)	$1,000 \sim 1,500 \Omega \cdot m$
Acidic alteration (kaolinite) rocks	Less than $1,000 \Omega \cdot m$

Table II-1-5 List of Resistivity and FE of Rock Samples

Sample No.	Location	Rock name	Resistivity ($\Omega \cdot m$)	FE (%)
1	Station 4	granodiorite	1,530	1.0
2	Station 5	holnfels	227,000	1.5
3	Station 11	holnfels	100,900	2.6
4	Station 14	fine-grained granodiorite	12,200	4.6
5	Station 24	fine-grained granodiorite (silicification)	6,390	4.0
6	Station 28	holnfels	127,000	3.0
7	Station 33	quartz bearing andesitic tuff (silicification)	15,000	2.1
8	Station 36	quartz bearing andesitic tuff	2,760	2.3
9	Station 39	holnfels	23,600	2.5
10	Station 41	quartz bearing andesite lava	113,000	2.6
11	Station 44	andesite lava (silicification)	805	1.6
12	Station 46	quartz bearing andesitic tuff	7,290	1.3
13	Station 49	quartz bearing andesitic tuff	2,120	2.4
14	Station 55	andesite lava (silicification)	11,500	1.5
15	Station 202	quartz bearing andesitic tuff	139	3.1
16	Station 401	granodiorite	7,720	3.2
17	Station 405	granodiorite	16,150	3.6
18	Station 413	grossular-quartz vein	2,660	0.5
19	MJE-1 200.0 m	granodiorite	5,320	2.9
20	MJE-1 300.0 m	granodiorite	2,270	5.4
21	MJE-2 100.4 m	granodiorite	896	1.8
22	MJE-2 190.0 m	granodiorite	1,500	4.6
23	MJE-2 300.0 m	granodiorite	13,170	0.6
24	MJE-2 273.5 m	granodiorite	1,060	7.3
25	MJE-2 291.0 m	granodiorite	3,830	5.4

In the relations between PFE value (0.3 to 3.0Hz are used) and sulfide contents in laboratory measurements of cores from MJE-1, 2 and 3 drill holes conducted in the El Torneado mineralized zone, PFE value tends to be higher as sulfide contents increase. An PFE value of 5 to 7% was obtained with 2 to 3% sulfide contents (by macroscopic observation).

Meanwhile, samples showing high PFE value contain little sulfide except "station 28" samples. The possibility of keeping microscopic pyrite could be through, for the trace of network of limonite and quartz are recognized.

Chargeability by time domain IP survey conducted in 1980 to MRME/DGGM in the same area was about 50mV in vicinities of MJE-2 and 3 drill holes (no measurements were taken near MJE-1). Samples of fresh rocks containing no sulfides showed an FE value of less than 2% with some exception. Since the chargeability of background by time domain IP survey is about 20mV, it can be said there is good correspondence between PFE value under frequency domain IP process and chargeability by time domain IP survey.

Comparative study of results of time domain IP survey and geological survey shows IP anomalous zones (where chargeability is more than 40mV) seen to extend along a northeastern direction, centering on the distribution area of the mineralized zone. Chargeability sharply decreases toward the south. On the northern side, the distribution of anomalous zones is not defined because IP survey lines were short. Vicinities of MJE-2 and 3 drill holes are situated in an IP anomalous zone of chargeability of more than 50mV, thereby suggesting the existence of strong alteration accompanying sulfides in the vicinities. However, sulfide dissemination is considered widely spreading in host rocks in adjacent mineralized zones based on the fact that IP anomalous zones are extensively observed around mineralized zones that are exposed on the ground surface.

(2) Apparent Resistivity Map

Using apparent resistivity values obtained at each measuring point, an apparent resistivity map was produced. The decay of electromagnetic wave becomes smaller as frequency drops. As will be noted from the fact that skin depth as a yardstick for penetration depth is given by $d = 503 \sqrt{\rho/f}$, apparent resistivity maps for lower frequency values better reflect resistivity structure at depths. In this report, apparent resistivity maps for 1,024, 256, 64 and 16Hz are shown in considering variations in apparent resistivity due to frequency (Fig. II-1-11 ~ Fig. II-1-14).

In major mineral showings, low and high apparent resistivities are observed in a pair and this characteristic is considered related to mineralization or alteration.

Low apparent resistivities were generally obtained at measuring points on the ridge near Bunque Roma including points 38, 39, 46, 56 and 58 but neither mineralization nor alteration was observed. It is generally known that the terrain effect appears on measurements at measuring points located on ridges, making the measurement values tend to become smaller than actual values. Moreover, this ridge runs in a direction nearly at a right angle to current dipole, i.e. the direction in which the ridge is mostly affected by topography. Therefore, it is considered that these low apparent resistivities are due to the terrain effect, and have no relation with mineralization or alteration.

The distribution of high and low apparent resistivities shows a trend for extension in northeastern to southwestern directions, and this is considered indicating the existence of a large geological structure that dominates the whole of this area.

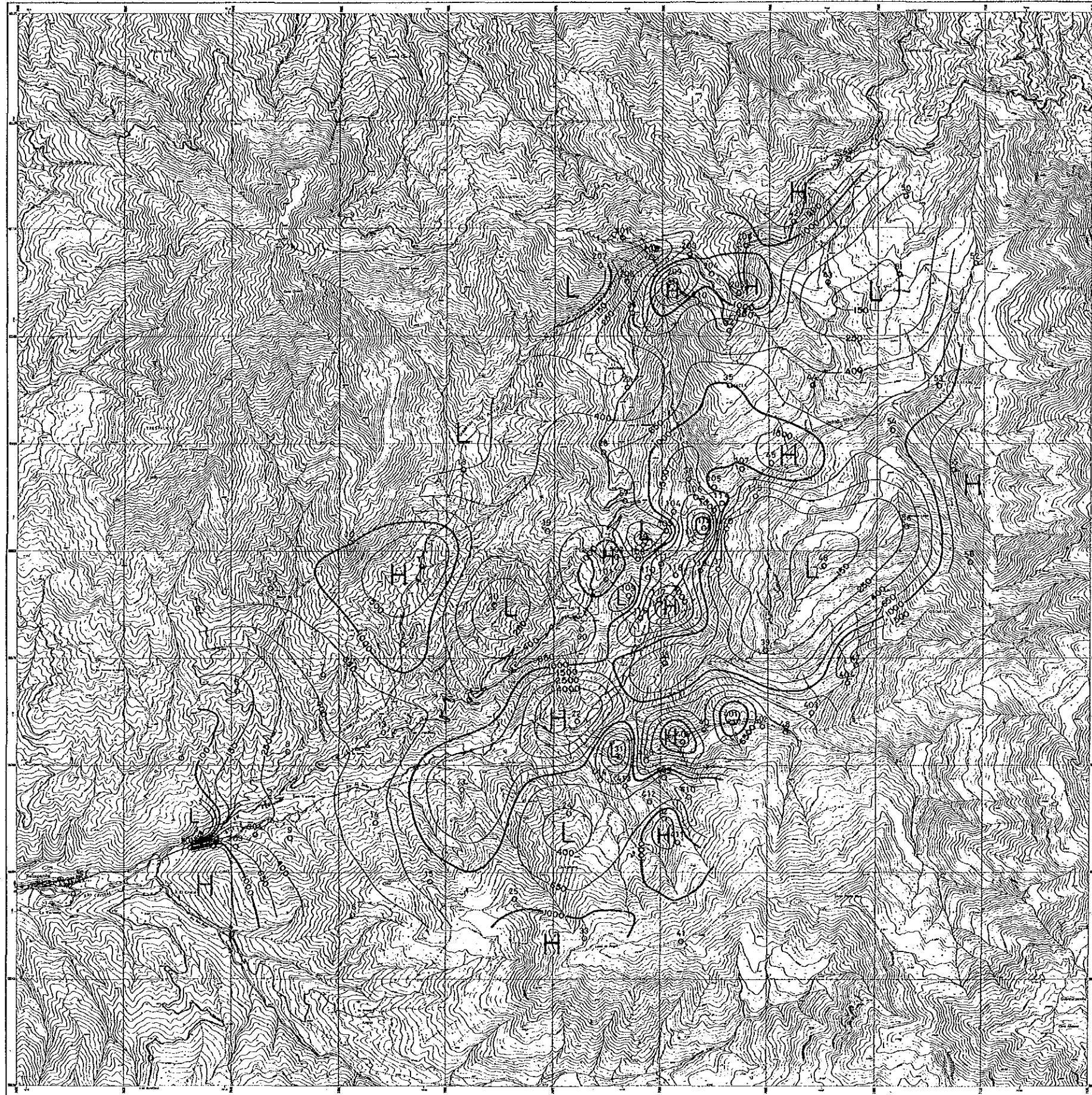
(3) Resistivity Structure Map

Based on thickness and resistivity obtained from one-dimensional multi-layered structure analysis conducted for each measuring point, resistivity structure maps for four levels, -100m G.L., -200m G.L., -500m G.L. and -1,000m G.L. (Fig. II-1-15 ~ Fig. II-1-18).

As a characteristic of the resistivity structure in principal mineral showings, it could be said that mineral showings occur on the boundary where low and high resistivities appear in a pair. To be specific, such boundary is seen around measuring points 29 and 108 in the El Torneado mineralized zone, 31 and 408 in the Osohuayco mineralized zone, and 3 and 301 in the El Cristal mineralized zone. Likewise, the boundary is seen around measuring points 202, 203 and 209 in the Las Palmas alteration zone. Furthermore, mineralized zones and alteration zones, which are located about the boundary of the Macuchi Formation and granodiorite, are found on the low resistivity side of this boundary.

Low resistivities in the boundary, extending to the depth are found at measuring point 29 only in the El Torneado mineralized zone. In the Osohuayco mineralized zone, low resistivities extend toward the southeast from the ground surface at measuring points 409 and 410 down to depths of measuring points 32 and 411. Meanwhile, in the El Cristal mineralized zone and the Las Palmas alteration zone, low resistivities are not distinctive at depths. Particularly at depths of the Las Palmas alteration zone, resistivity is not low. Consequently, it is possible that mineralization and alteration in this zone are limited at the shallow part only. Furthermore, besides the above mineral showings, measuring points 11, 19 and 20 can be cited as the boundary with a pair of low and high resistivities. This boundary is an interesting area because the alteration zone of Las Juntas was observed. However, only measuring point 11 shows a high resistivity

BALZAPAMBA



LEGEND

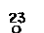

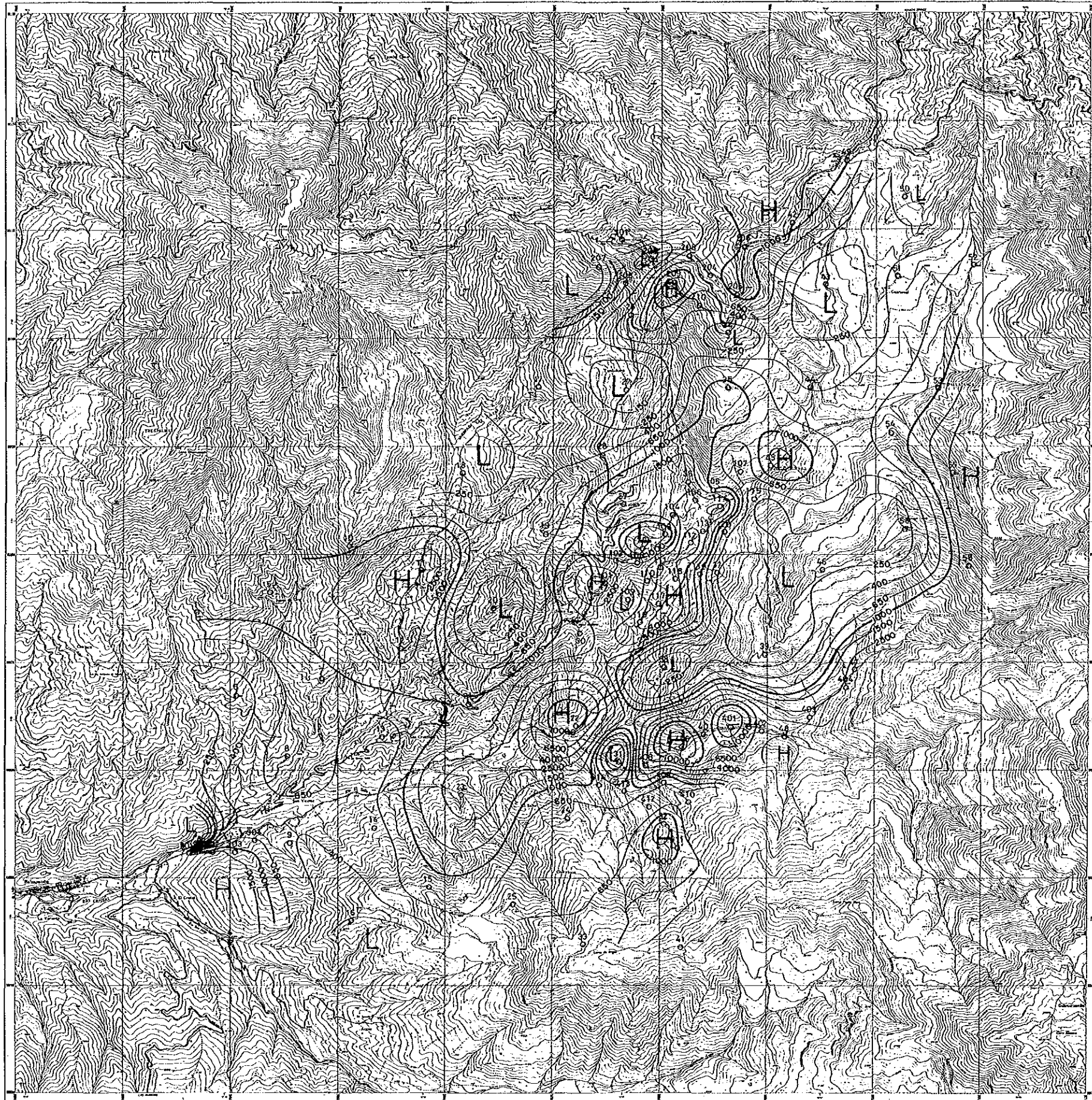
-  Station and No.
-  Apparent Resistivity Contour ($\Omega \cdot m$)
- H** High Apparent Resistivity
- L** Low Apparent Resistivity

Fig. II-1-11 Apparent Resistivity Plan Map(1,024Hz)

BALZAPAMBA



LEGEND

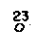

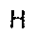

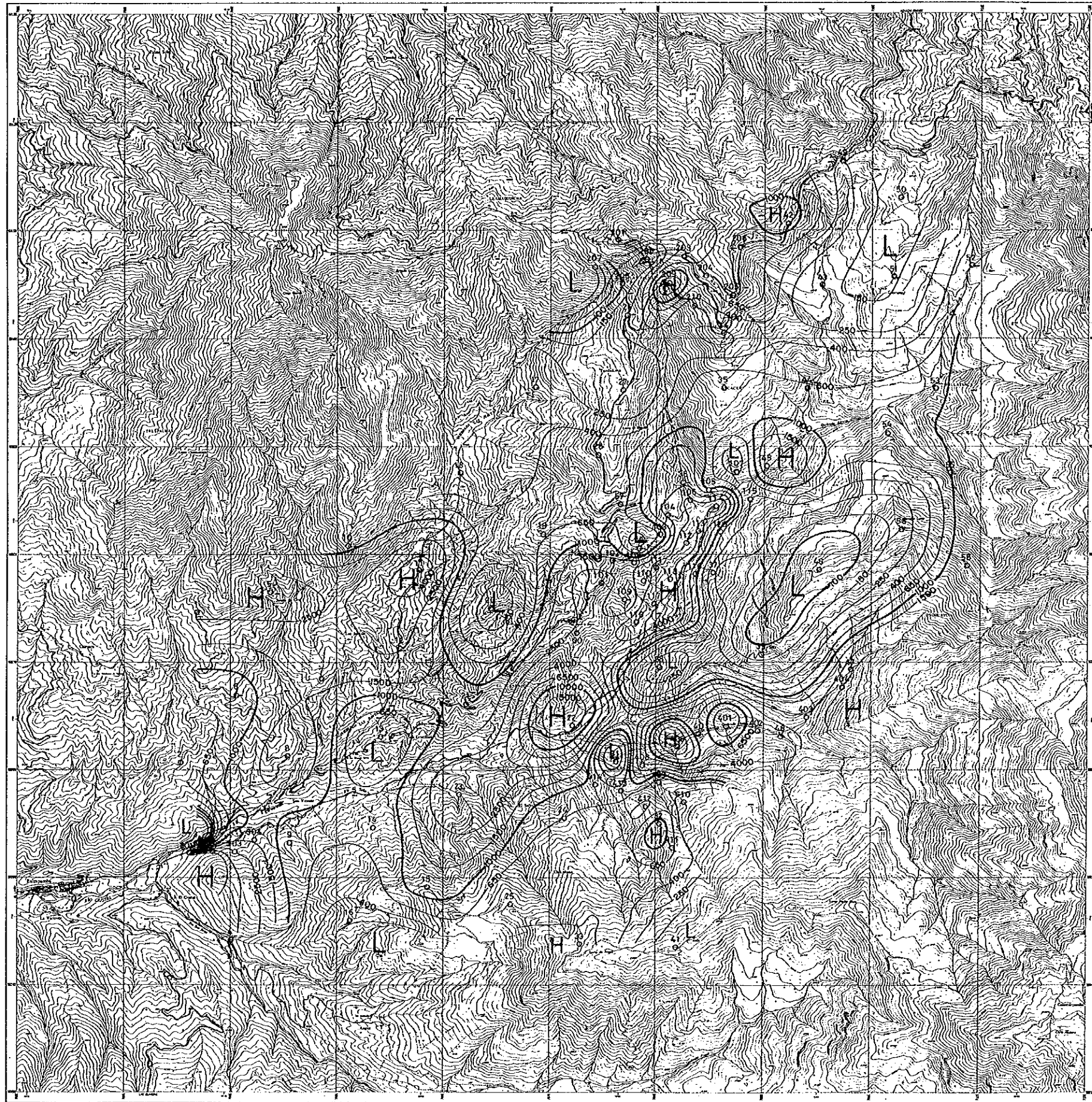
-  Station and No.
-  Apparent Resistivity Contour ($\Omega\cdot m$)
-  High Apparent Resistivity
-  Low Apparent Resistivity

Fig. II-1-12 Apparent Resistivity Plan Map (256Hz)

BALZAPAMBA



LEGEND

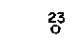
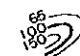
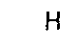

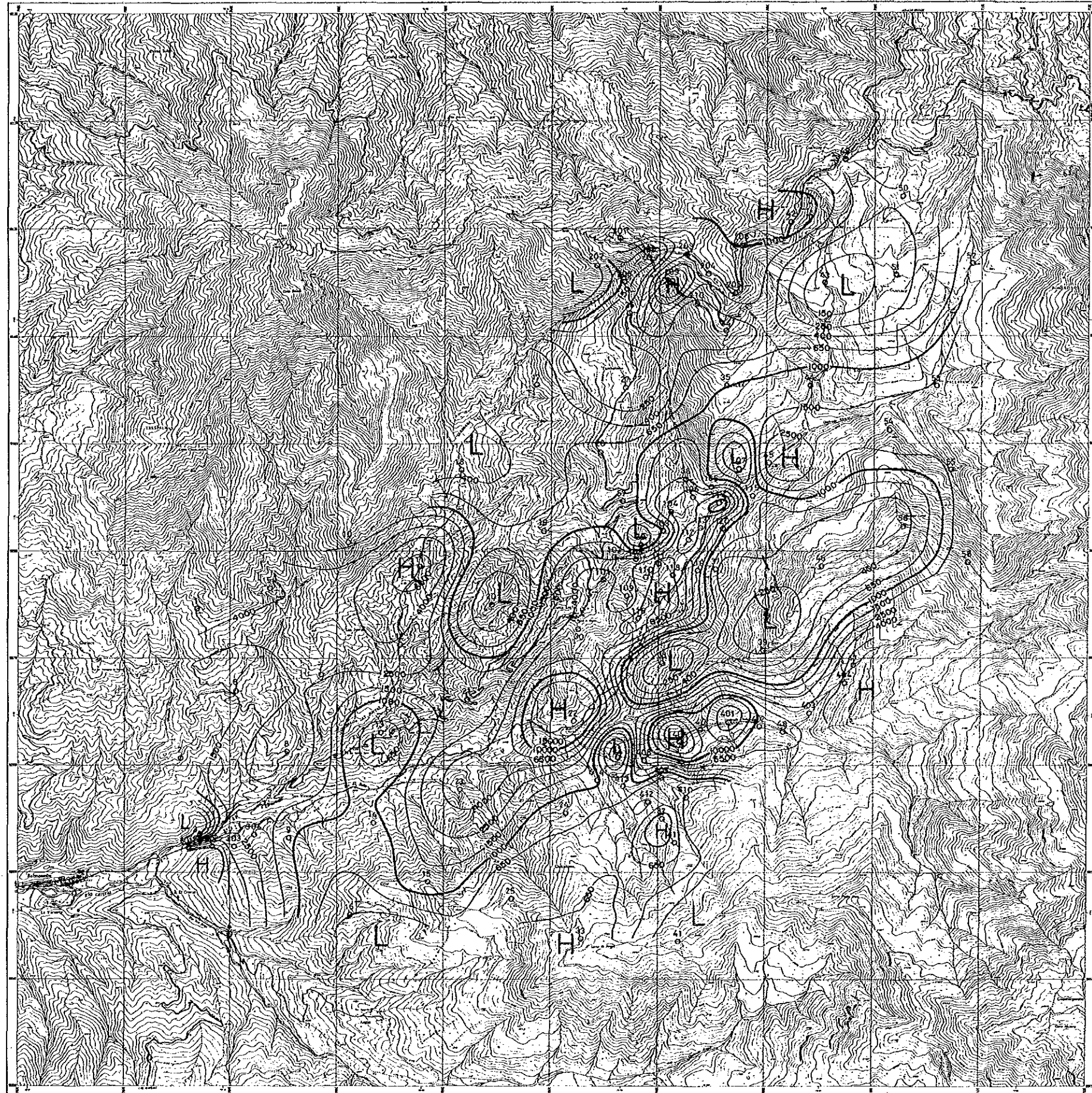
-  Station and No.
-  Apparent Resistivity Contour (Ω-m)
-  H High Apparent Resistivity
-  L Low Apparent Resistivity



Fig. II - 1 - 13 Apparent Resistivity Plan Map (64Hz)

BALZAPAMBA



LEGEND

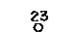

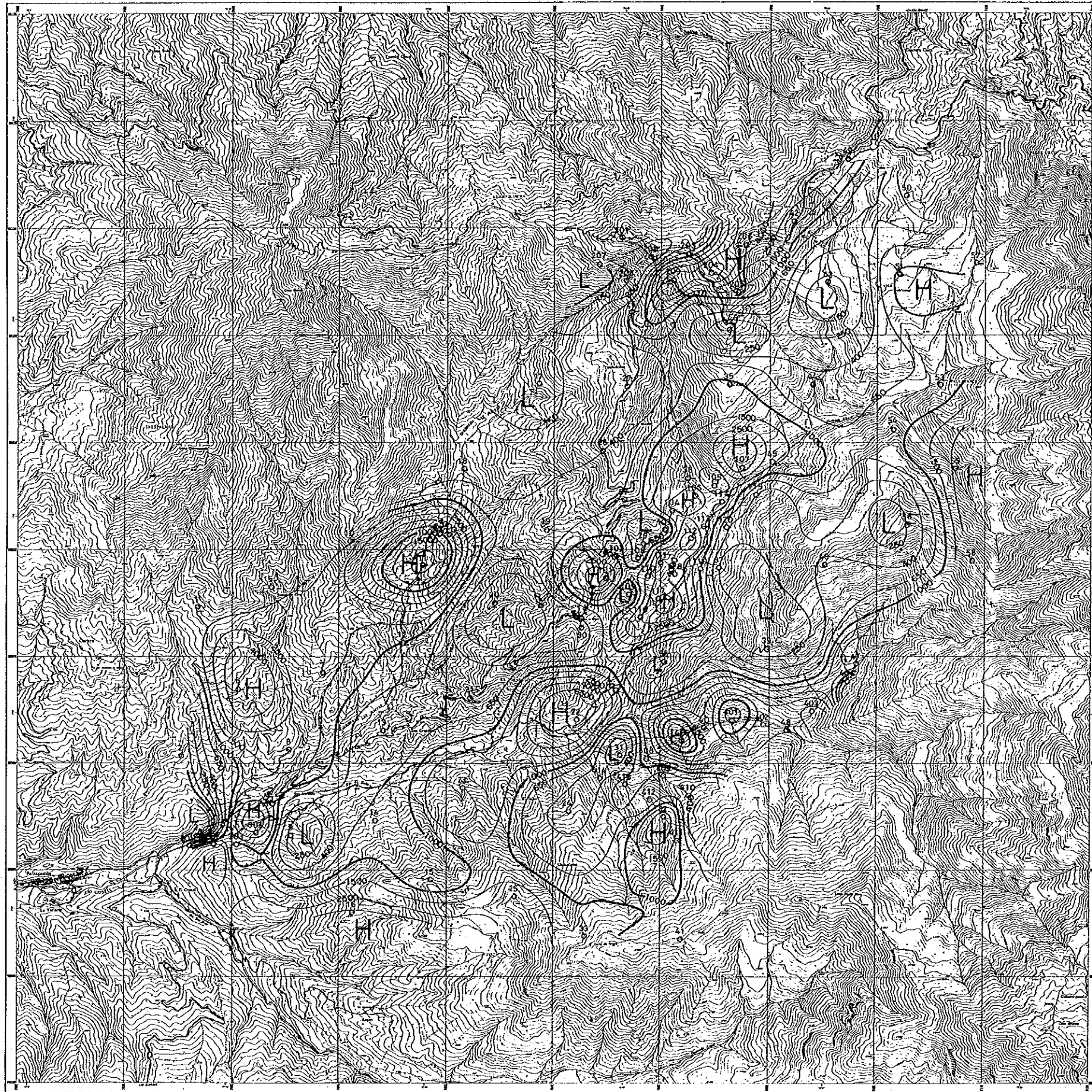
-  Station and No.
-  Apparent Resistivity Contour ($\Omega\cdot m$)
- H** High Apparent Resistivity
- L** Low Apparent Resistivity

Fig. II-1-14 Apparent Resistivity Plan Map(16Hz)

BALZAPAMBA



LEGEND

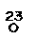

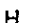

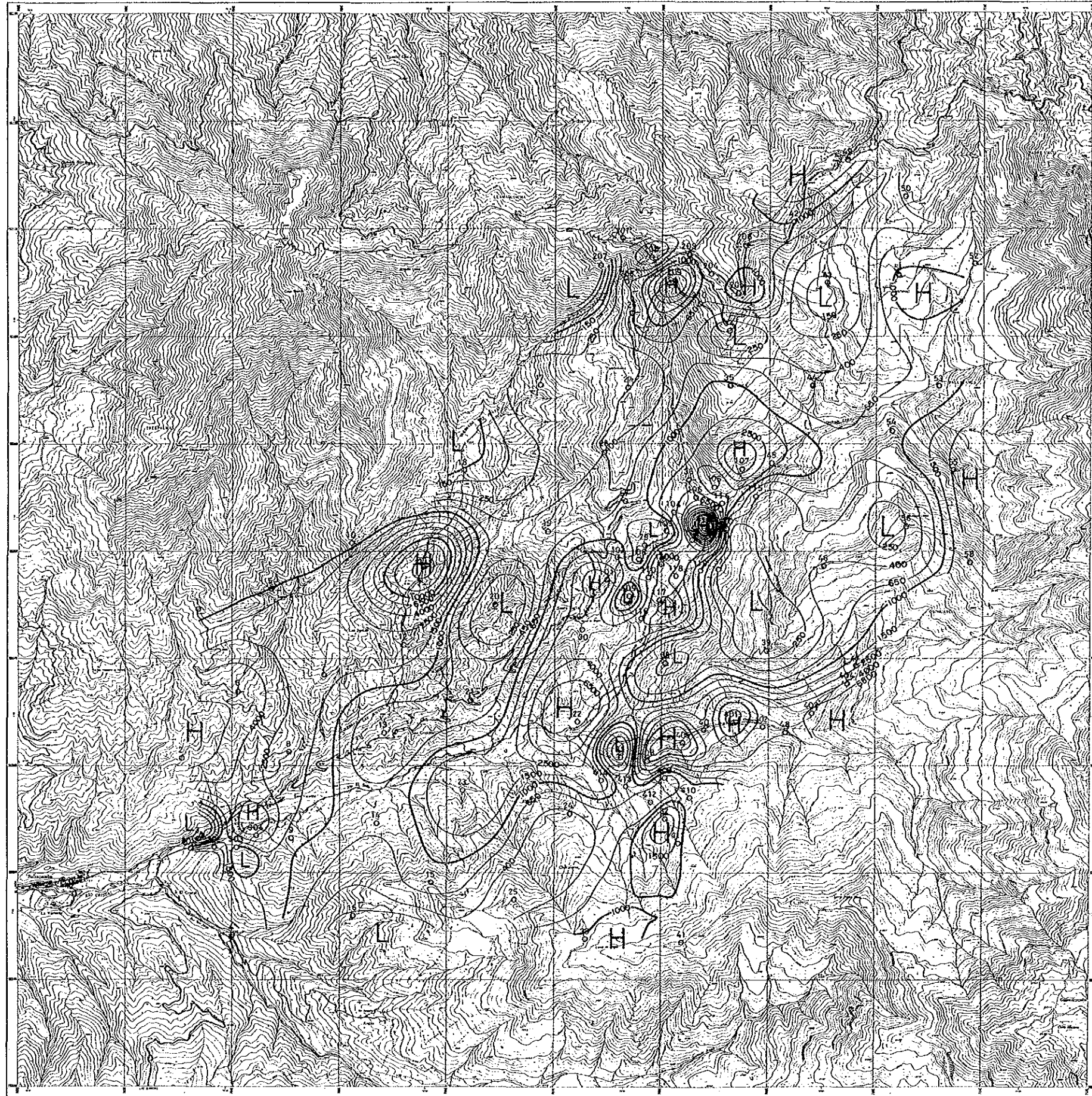
-  Station and No.
-  Analyzed Resistivity Contour ($\Omega \cdot m$)
-  High Analyzed Resistivity
-  Low Analyzed Resistivity



Fig. II-1-15 Analyzed Resistivity Plan Map (100m depth)

BALZAPAMBA



LEGEND

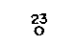

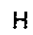

-  Station and No.
-  Analyzed Resistivity Contour ($\Omega \cdot m$)
-  High Analyzed Resistivity
-  Low Analyzed Resistivity

Fig. II-1-16 Analyzed Resistivity Plan Map(200m depth)

